

Synthesis of CuO Nanoparticles using *Amorphophallus paeoniifolius* Tuber extract and its photo-catalytic activity on Malachite Green dye

Anbarasan V.¹, Arivalagan K.², Alvin Kalicharan A.³ and Kistan A.^{3*}

1. Department of Chemistry, DMI College of Engineering (Autonomous), Chennai-600123, INDIA

2. Department of Chemistry, Government Arts College for Men (A) Nandanam, Chennai-600035, INDIA

3. Department of Chemistry, Panimalar Engineering College (Autonomous), Chennai-600123, INDIA

*vishmikrish@gmail.com

Abstract

The present study carried out Equilibrium, Kinetics and Thermodynamic studies for the removal of Malachite Green dye by Green Synthesized Copper Oxide Nanoparticles (*Amorphophallus paeoniifolius* Tuber). The synthesized copper oxide nanoparticles were characterized by Ultraviolet Vis spectroscopy (UV-Vis), X-ray Diffraction (XRD), Fourier Transform Infrared Spectroscopy (FT-IR), Scanning Electron Microscope (SEM), Transmission Electron Microscope (TEM) and Energy Dispersive X-ray (EDX). Adsorption parameters such as initial dye concentration, adsorbent dosage, pH and contact time were used.

Pseudo first order and second order kinetics parameters were also calculated. It is a very simple green chemical strategy, low-cost and effective alternative method. This method is cost-effective in terms of energy, time and easiness. This procedure resulted in the production of copper oxide Nanoparticles on a huge scale.

Keywords: *Amorphophallus paeoniifolius* tuber, CuO NP's, Malachite green dye, Colour degradation, Pseudo first order kinetics.

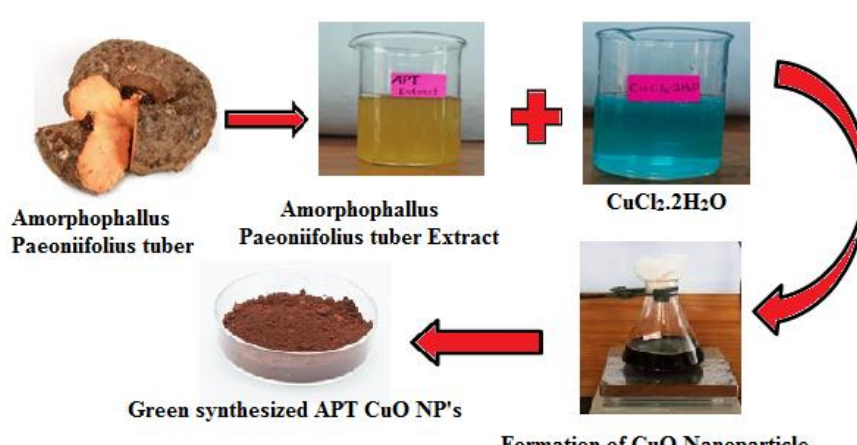
Introduction

The discharge of effluents of azo dyes into the water is uncontrollable because the dyes degrade to carcinogenic and

toxic products. Among a wide array of methods employed for the treatment of wastewater, adsorption has received many attentions since it is simple, cost effective and reliable. Hence, seeking for effective adsorbents is increasingly enhancing because the majority of widely used adsorbent materials are very expensive, difficult to recover and recycle and also need high cost for activation and reactivation^{5,38,40}.

The synthesis process of nanomaterial and the investigation of their applications and properties are one of the inspiring parts of the advanced scientific research. Different physical and chemical methods are used for the synthesis of metal oxide nanoparticles; however, the conventionally used methods such as sol-gel, chemical reduction and hydrothermal are costly methods and non-eco-friendly by producing toxic chemicals as end products. Thus, eco-friendly methods for the synthesis of metal oxide nanoparticles attracted the attention such as the use of plant extract, microorganisms and algae. Plant extracts are involved in redox reactions which reduce metal ions to form nanoparticles. Metabolites such as sugars, terpenoids, polyphenols, alkaloids, phenolic acids and proteins play essential roles in the reduction of metal ions to nanoparticles and support the stability of nanoparticle^{8,27}.

Based on the previous literature reports, nanoparticles were synthesized from various plants extracts such as *Acalypha indica*, *Phyllanthus amarus*, *Terminalia arjuna*, *Calotropis gigantean*, *Malva sylvestris*, *Cassia alata*, *Gloriosa superba* and *Carica papaya* and their antimicrobial activities were also reported^{10,15,16}.



Graphical Abstract

In the present study, *Amorphophallus paeoniifolius* tuber extracts were considered for the synthesis of nanoparticles. *Amorphophallus paeoniifolius* is an herbaceous, perennial C3 crop is categorized under the family Araceae; it has yellow flesh and is a rich source of starch. This plant is also known as an elephant foot yam and has the local name, "Karunai Kizhangu". This plant is widely available in Bangladesh at very low cost. This medicinal plant contains different phytochemical components such as steroids, flavonoids, carbohydrates, tannins, saponins and proteins^{21,25,37}.

Due to the presence of different bioactive molecules, this plant has many uses in medicinal purposes such as cough, vomiting, bronchitis, asthma and anorexia. Besides these medicinal uses, the above-mentioned phytochemicals in this plant can be used for synthesizing metal nanoparticles by reducing metal ions. A recent work reported synthesis of AgNP's by using tuber extract of *Amorphophallus paeoniifolius* and their potential antibacterial activity¹⁸.

In this study, we reported cost-effective, simple, rapid and eco-friendly synthesis of CuO NP's at room temperature. Tuber extract (without bark) of *Amorphophallus paeoniifolius* was used as the source of reducing and stabilizing agents. Using this tuber extract as a reducing and stabilizing agent, instead of toxic chemicals, satisfies the main object of green chemistry^{15,17}.

Material and Methods

Preparation of Malachite Green Solution: Malachite green (MG) dye has chemical formula C₂₃H₂₅N₂Cl (molecular weight = 364.92, λ max = 617nm)¹². Analytical reagents were used without any further purification in addition to deionised water, copper chloride di-hydrate

(CuCl₂.2H₂O) Sodium hydroxide, hydrochloric acid and ethanol.

Preparation of *Amorphophallus paeoniifolius* Tuber extract: *Amorphophallus Paeoniifolius* tuber was collected from near vegetable market in Chennai (Tamilnadu), cleaned from suspended dirt and mud and washed with water several times and thrashed into small species and dried in sunlight for 4 days. The dried tuber was ground with an electric grinder and stored. 10g of this powder was added to (200 ml) distilled water and boiled for 15 minutes. The colour of solution change into brown. The obtained solution cooled at room temperature and filtered. Centrifuge the filtrate at 1200rpm for 10 minutes and then adjust at pH 12 and store the extract at room temperature until use.

Preparation Copper Oxide Nanoparticles: Take 50ml of *Amorphophallus paeoniifolius* tuber extract and add 0.1M of copper chloride di-hydrate (CuCl₂. 2H₂O) solution at room temperature, where the colour changed from light blue to yellowish grey. It was then filtered and dried in electrical oven for 24 hours at 100°C. The dried sample was kept in Muffle furnace for 4 hours at 500°C. The green synthesized CuO NP's are formed at uniform particle size and stored for further characterization and uses.

Preparation of Adsorbate: The synthetic dye such as malachite green (MG) was purchased from Kevin laboratories in Chennai. A stock solution of (1000mg/L) was prepared by dissolving 1.0 g of dye distilled water. Distilled water was used for preparing all the solution and reagents.

The percentage of removal of colour from dye solution is determined by the following formula¹⁹:

$$\% \text{ removal of colour} = \frac{(C_0 - C_e)}{C_0} \times 100 \quad (1)$$

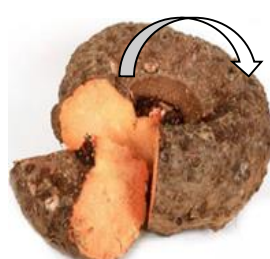


Fig. 1: *Amorphophallus Paeoniifolius* Tuber extract

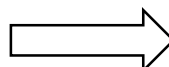


Fig. 2: Green synthesized APT CuO Nanoparticle

The maximum MG uptake q_e (in mg g^{-1}) was calculated as:

$$q_e = \frac{(C_0 - C_e)V}{M} \quad (2)$$

where C_0 and C_e are initial and final MG concentrations in mg/L respectively W is the amount of CuO NP (in g) and V is the volume of MG solution.

Results and Discussion

UV- Visible Adsorption Spectroscopy for copper oxide nanoparticles: The green approach for the formation of copper oxide nanoparticles using *Amorphophallus paeoniifolius* tuber extract was reported. UV-Vis spectroscopy was used to monitor the process of the bio reduction of $\text{CuCl}_2 \cdot 2\text{H}_2\text{O}$ to CuO nanoparticles and to monitor the formation and optimization of CuO NP's. Color change was the first-hand information for the formation of CuO NP's which was further confirmed by the appearance of characteristic Surface Plasmon Resonance (SPR) peak between 206 to 212 nm. Fig. 3 shows the UV-Visible absorption spectrum of copper oxide nanoparticle. The spectrum showed the absorbance peak at 242 nm corresponding to the characteristic band of copper oxide nanoparticle^{17,20}.

Fourier Transform Infrared (FT-IR) Spectroscopy: FT-IR analysis was used to investigate the presence of some functional groups in both the APTE and the synthesized CuO NP's which are responsible for reducing as well as capping agent. Fig. 4 showed the FT-IR absorption spectra of green synthesized CuO NP's and APTE in the range of 400 cm^{-1} to 4000 cm^{-1} . Absorbance bands at 3248, 2127, 1362 and 752 cm^{-1} were observed in the spectrum of *Amorphophallus paeoniifolius* tuber extract. A broad band at 3248 cm^{-1} was due to the O-H stretching of alcohol compounds. The peaks at 1827 and 1363 cm^{-1} are containing $-\text{NH}_2$ group and $\text{C}=\text{O}$ groups of flavonoids¹¹. 775 cm^{-1} peak is due to C-H bonds. FTIR spectrum of CuO NP's for the peaks appeared at 3393, 1632, 1015, 709 and 562 cm^{-1} . The peaks at 3393, 1632 and 1015 cm^{-1} correspond to hydroxyl group (-OH) stretching,

hydroxyl (-OH) bending and C-O stretching respectively. The narrow bands at 562 confirm the formation of CuO NP's.

XRD pattern analysis: The copper oxide nanoparticles were synthesized by using the green method from plant *Amorphophallus paeoniifolius* tuber extract. To evaluate the crystalline structure, size and purity of the prepared CuO NP's, the XRD analysis was performed³⁹. Figure 5 shows diffraction peaks for green synthesized CuO NP's noticed at 2θ values of Brags angle for 33.4° (110), 35.4° (002), 38.8° (111), 48.2° (200), 55.23° (202), 59.3° (020) and 62.2° (202) respectively and were used to characterize the monoclinic structure of CuO NP's³⁹.

The average particle size of synthesized copper oxide nanoparticles was calculated using Debye- Scherrer's formula^{25,27}:

$$D = 0.9\lambda / \beta \cos \theta \quad (3)$$

A sharp peak at $2\theta = 35.4$ and 38.8 with the diffraction of the (022) and (111) plane indicates that confirmation of CuO NP's. The average crystallite size in the samples of CuO NP's is below 38.91 nm .

Scanning electron microscope (SEM) analysis: The morphology and surface structure of the synthesized CuO NP's were analysed using SEM and obtained micrograph is shown in fig. 6. The shape of the nanoparticle was nearly spherical, with less evidence of agglomeration. Previous studies confirmed CuO NP's spherical shape^{28,29}. The average particle size determination using image J software showed that the average particle size was 59.99 nm . The particle size distribution for CuO NP's obtained in this study agreed with previous studies^{24,30,36}.

Energy Dispersive X-Ray Diffractive (EDAX) Analysis: To gain further insight into the features of the green synthesized CuO NP's, the chemical composition of the NP's was analysed using EDAX (Fig. 7).

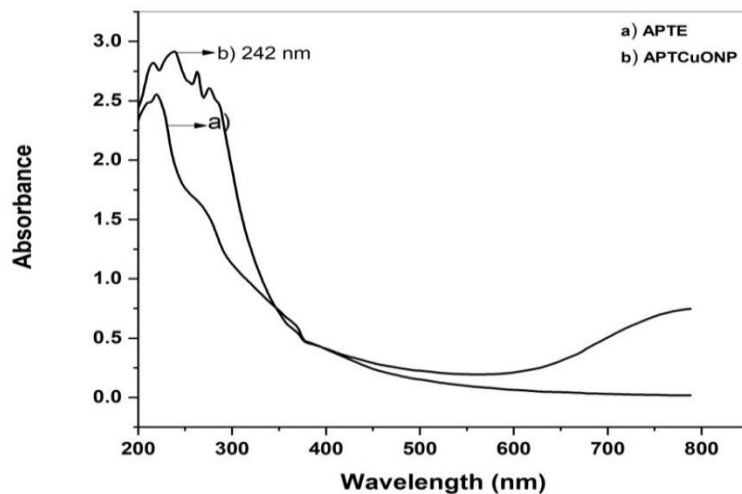


Fig. 3: UV-visible adsorption spectrum of a) APTE and b) APT CuO NP's

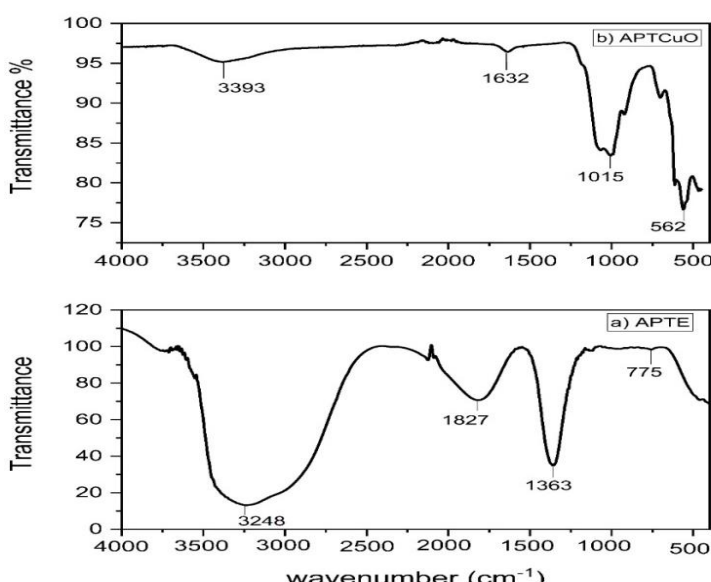


Fig. 4: FTIR Spectrum of a) *Amorphophallus Paeoniifolius* tuber b) CuO NP's

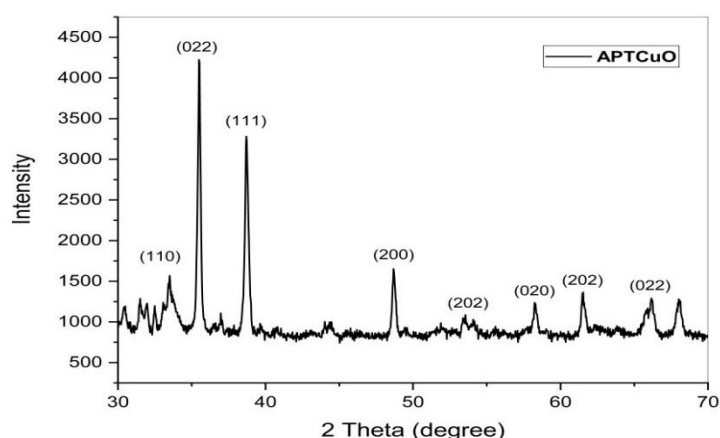


Fig. 5: X-ray diffraction pattern of APT extract-mediated synthesized CuO NP's

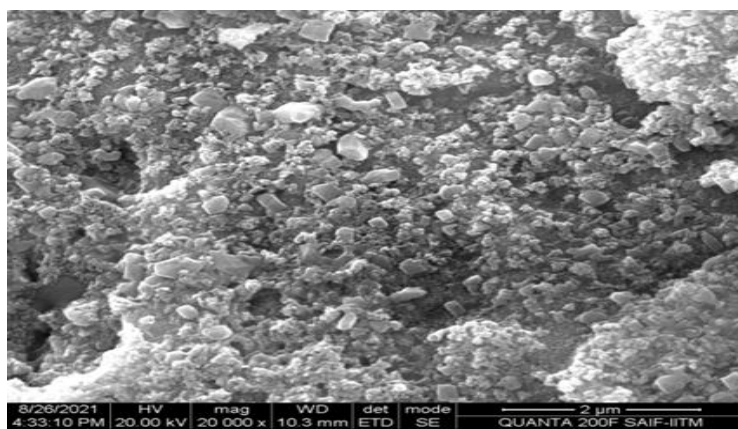


Fig. 6: SEM image of Green synthesized copper oxide nanoparticles

The energy-dispersive spectra of the samples obtained from the SEM-EDS revealed that the sample prepared by using *Amorphophallus Paeoniifolius* tuber extract has pure CuO phases. The results indicate that the reaction product is composed of high purity CuO NP's which agrees with the result obtained from XRD. The weight composition obtained from EDAX analysis of the normalized spectrum was Cu (78.07%) and oxygen (21.93%). EDAX also revealed the

formation of nonstoichiometric CuO NP's with oxygen vacancy which could lead to better antibacterial activity^{23,28}.

Transmission Electron Microscope (TEM): The detailed morphological and size analyses of green synthesized copper oxide nanoparticles were studied using electron microscope and results are shown in fig. 8. The TEM image reveals that the biosynthesis CuO NP's agglomerated interconnected to

each other and are spherical in shape which is also in agreement with result obtained from SEM. The particle is found to be between 10-60 nm. The particle size was calculated by histogram.

Effect of pH solution: The initial pH of the working solution was adjusted between 3-10 by addition of HCl and NaOH solution. Fig. 9 shows the effect of pH on the adsorption of MG by GS-APTCuONP. The percentage removal increased with increasing pH = 3 to pH = 7 and thereafter slightly decreased 8 to 10 due to attained equilibrium. GS-APTCuO NP's had maximum dye adsorption 99% at pH 7. It can be seen that dye adsorption was unfavourable in pH <4. The decrease in the adsorption with decrease in pH may be attributed to two reasons. As the pH of the system decreased, the number of -ve charged adsorbent sites decreased and the number of +ve charged surface sites increased, which did not favour the adsorption of +ve charged dye cations due to electrostatic repulsion^{3,9,31}. While increasing pH, positively charged cationic dye becomes dominant.

Effect of adsorbent dosage: Adsorbent dosage also plays an important role in the adsorption process because it determines the capacity of an adsorbent for a given initial concentration of the adsorbate. The effect of adsorbent dosage was studied. The other parameters were fixed; the

dosage utilized was varied from 0.2 to 1.0 g against a solution volume of 50 mg/L MG dye.

The fraction of adsorbed colorant intensified with cumulative adsorbent quantity owing to increased availability of sorption sites and surface area. The results are shown in fig. 10. The amount of MG dye removal increased with increase in adsorbent dosage from 0.2 g to 0.8. Thereafter, the percentage of dye removal decreased. The maximum sorption was obtained at 0.8g. The % of porosity increased by increasing adsorbent dosage.

Effect of initial dye concentration of Malachite green: The initial concentration of dye has a very important role in adsorption phenomena.

The inference of the initial concentration of MG in the solutions on the rate of adsorption on APT CuO NP's was investigated. Dye range 10–50 (mg/L) was studied and output is depicted in figure 11. The adsorption capacity of GS-APT CuO NP's decreased by increasing initial dye concentration 10 to 50 mg/L. Maximum adsorption of 98.94% was recorded for 10mg/l and then the percentage removal decreased till the adsorption attains the equilibrium. It means that the adsorption is highly dependent on initial concentration of Malachite green.

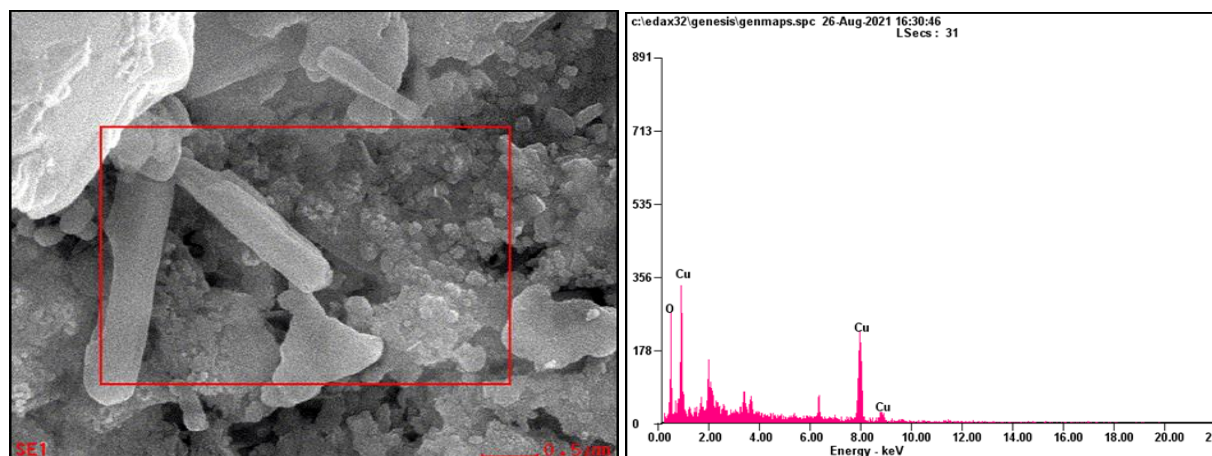


Fig. 7: EDAX spectrum of copper oxide nanoparticles

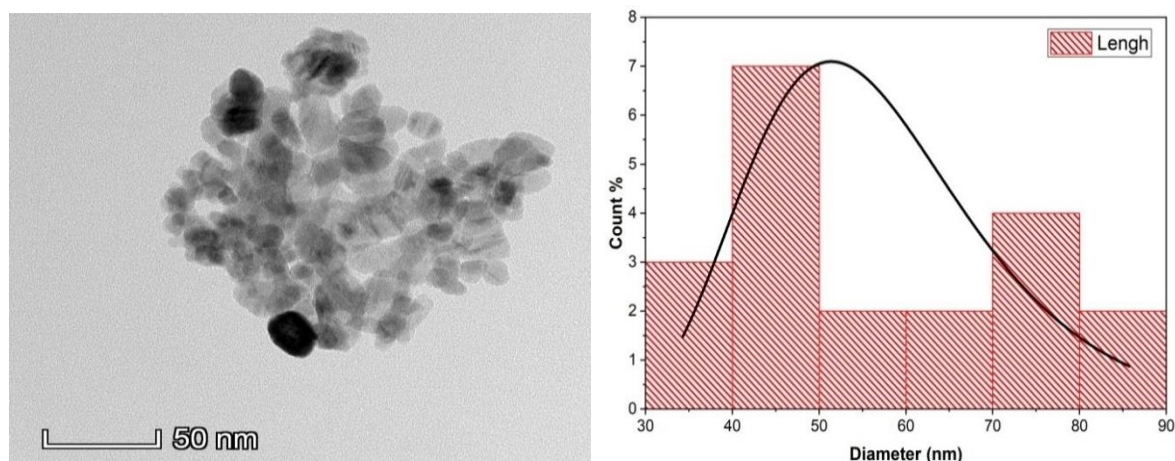


Fig. 8: a) HR-TEM image b) Histogram of APT copper oxide nanoparticles

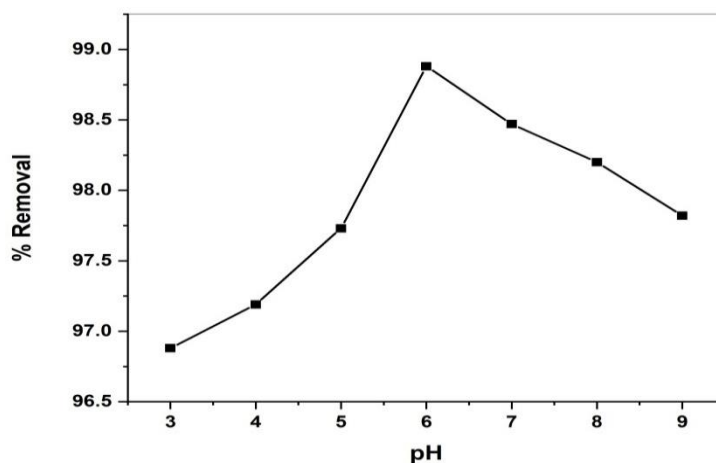


Fig. 9: Effect pH on the adsorption of Malachite green onto GS-APTCuO NP's

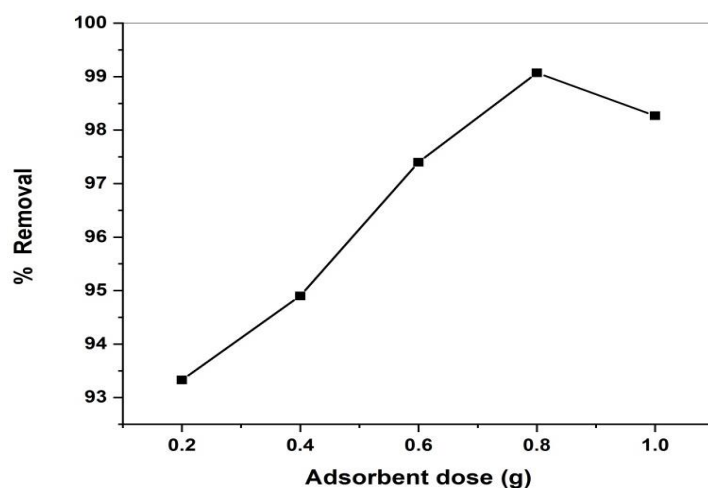


Fig. 10: Effect of adsorbent dose on removal of Malachite green

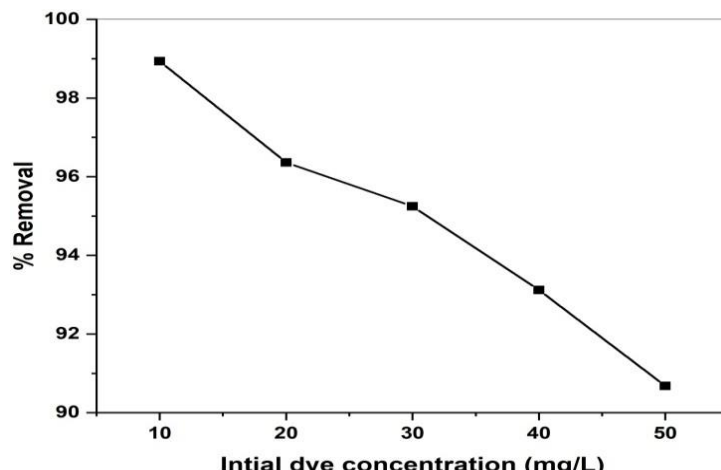


Fig. 11: Effect of Initial MG dye concentration on the adsorption of GS-APTCuO NP's

Since the adsorbent dose is fixed, there are a fixed number of active sites as a result percentage removal decreased with increasing concentration. At low initial concentrations of MG dye, relatively high percentage sorption were observed. As a result of the high ratio of adsorbent surface binding sites to the dye concentration, a fewer number of dye molecules were competing for the available binding sites on the adsorbent^{2,29,35}. The increase in the initial concentration of

the dye enhances the interaction between the dye molecules and the surface of the adsorbent²⁶.

Effect of contact time: Equilibrium time is one of the most important parameters in the design of economical waste treatment system and its effect on the adsorption of MG on APT-CuO NP's is presented. These experiments have been carried out at variation time of contact (30-150 minutes).

After every contact time, one sample was removed and filtered immediately and the filtrate was analysed (Fig. 12). The amount adsorbed first rapidly increased and then gradually decreased until equilibrium was reached. This is perhaps due to the initial availability of maximum number of active sites which gets saturated with time. The removal efficiency was found to be in the range of 95.47.1 to 98.8% when the time rises from 30 to 60 minutes respectively and then gradually decreased with increasing time from 60 to 150 minutes. The result showed that the prepared adsorbent has short equilibrium time which shows that the adsorbent has enough number of active site for a given concentration. In fact, short equilibrium time is recommended on the view of water treatment technologies^{6,14}.

Effect of temperature: The temperature can affect adsorption rate. In this study, the effect of temperature on MG adsorption was investigated in the range of 298–328 K (Fig. 13). The adsorption of dye decreased with increase of temperature. The percentage removal adsorption decreased from 98.97% to 97.76% and the temperature increased from 298K to 328K. The decrease dye adsorption at higher temperature was due to the weakening supportive between

active site on the adsorbent and adsorbate^{1,4,33}. The adsorption process is exothermic and MG dye adsorption onto CuO NP's occurred mainly by physico-adsorption²².

Adsorption kinetic studies: The pseudo-first order and pseudo-second-order models were used to investigate the adsorption kinetics of the MG dye on CuO NP's.

a) Pseudo-first-order method: The pseudo-first—order rate model of Lagergren's is based on solid capacity and is generally expressed as follows:

$$\log (q_e - q_t) = \log q_e - K_1/2.303t \quad (4)$$

where q_e is the amount of solute adsorbed at equilibrium per unit weight of adsorbed (mg/g), q_t is the amount of solute adsorption at any time (mg/g) and K is the adsorption constant. This expression is the most popular form of the pseudo first order kinetics model. K_1 values at different initial MG concentration were calculated from the plots of $\ln(q_e - q_t)$ vs t . Constant K_1 and correlation coefficient (R^2) were calculated and summarized in table 1. This model has very poor correlation coefficients $R^2 = 0.8027$.

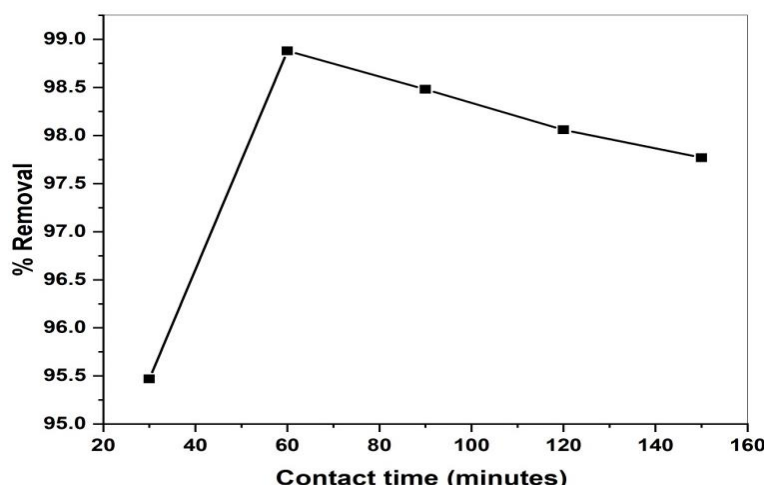


Fig. 12: Effect of contact time on the adsorption of MG onto GS-CuO NP's

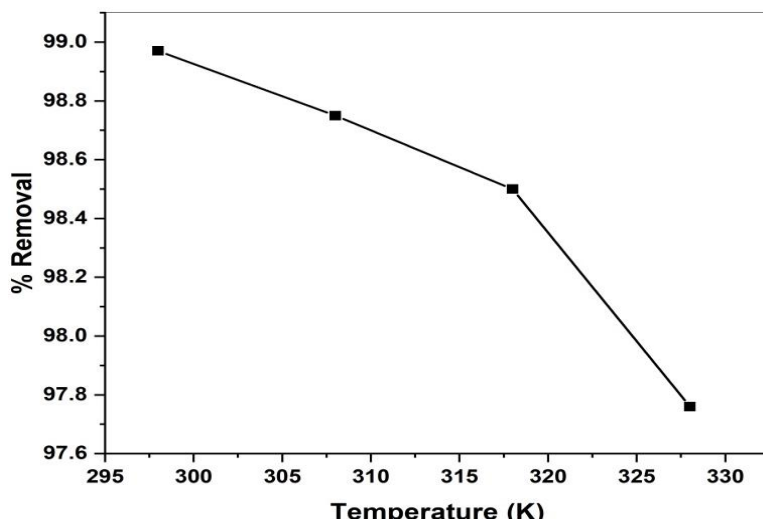


Fig. 13: Effect of temperature on the adsorption of MG onto GS-APT CuO NP's

b) Pseudo-Second-Order Model: The kinetics data were analysed using the pseudo –second-order model which can be expressed as follows:

$$t/qt = 1/K_2 q_e^2 + t/q_e \quad (5)$$

The plot of $1/qt$ vs t should give a linear relationship from which q_e and K_2 can be determined from the slope and intercept of the plot. The pseudo-second-order rate constant K_2 and q_e determined from the model as well as correlation coefficient are presented in table 1. The observed R^2 (0.9981) values are very high for the pseudo-second-order kinetic model where the values of q_e _{cal} are in good agreement with q_e _{exp}. It is therefore evident that pseudo-

second-order model is the best fit kinetic model in describing the adsorption process MG onto GS-CuO NP's.

Conclusion

In this report, we discussed a green, rapid, one-pot synthesis of CuO NP's, $\text{CuCl}_2 \cdot 2\text{H}_2\text{O}$ was used as a source of Cu and tuber extract of *Amorphophallus paeoniifolius* was used as reducing and stabilizing agent in this synthesis pathway. The CuO NP's were characterized by UV-visible, FT-IR, XRD, SEM-EDX and TEM. The results showed that the adsorption followed pseudo-second-order for sorption of MG onto green synthesised CuO NP's. In the present work, the green method is very simple, economic and eco-friendly.

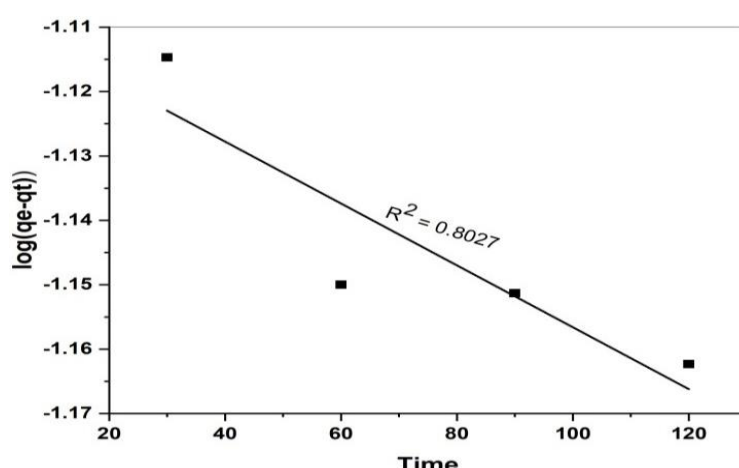


Fig. 14: Pseudo-first-order kinetic model plot for adsorption of MG onto GS-CuO NP's

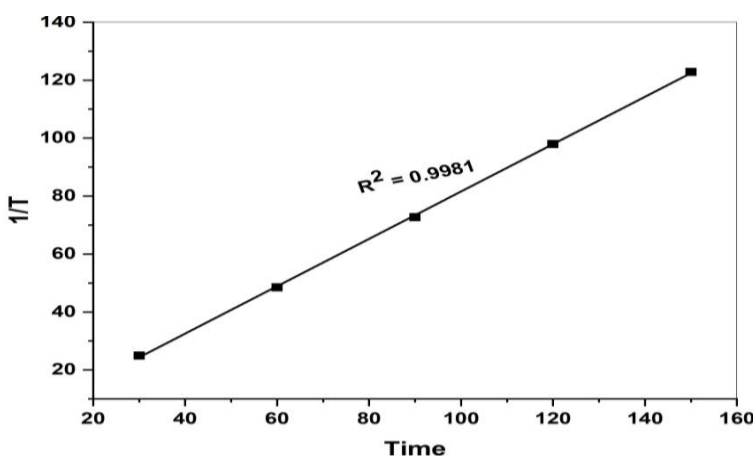


Fig. 15: Pseudo-second order kinetic model for adsorption of the MG onto GS-CuO

Table 1
Adsorption kinetics of MG

Adsorption Kinetics	Parameters	Malachite Green
Pseudo First Order	K_1 (min ⁻¹)	0.0011
	q_e (mg g ⁻¹)	0.0778
	R^2	0.8027
Pseudo Second Order	h (g ⁻¹ mg ⁻¹ min ⁻¹)	6.0060
	q_e (mg g ⁻¹)	1.2235
	R^2	0.9981

The synthesized nanoparticle could be a good alternative for the removal of malachite green colour (MG) from aqueous solution very efficiently.

References

1. Acharyulu N.P.S., Dubey R.S., Swaminadham V. and Pammi S.V.N., Green synthesis of CuO nanoparticles using *Phyllanthus amarus* leaf extract and their antibacterial activity against multidrug resistance bacteria, *International Journal of Engineering Research & Technology*, **3**, 255–258 (2014)
2. Altikatoglu M., Attar A., Erci F., Cristache C.M. and Isildak I., Green synthesis of copper oxide nanoparticles using *ocimum basilicum* extract and their antibacterial activity, *Fresenius Environ. Bull.*, **25**, 7832–7837 (2017)
3. Amal M.I., Ghaida H.M. and Laila M., A Copper (II) oxide Nano catalyst preparation and characterization: green chemistry route, *Bull. Natl. Res. Cent.*, **42**, 6 (2018)
4. Amin F. et al, Green synthesis of copper oxide nanoparticles using *Aerva javanica* Leaf extract and their characterization and investigation of in vitro antimicrobial potential and cytotoxic activities, *Evid. Based Complement. Altern.*, **34239581**, 1-12 (2021)
5. Awwad A.M., Albiss B.A. and Salem N.M., Antibacterial activity of synthesized copper oxide nanoparticles using *Malva sylvestris* leaf extract, *Sikkim Manipal University Medical Journal*, **2**, 18–25 (2015)
6. Aziz L.M., Wissam Qadry Mutaab Alqaissy and Ban M.A. Alani, Effect of carbon nano colloid and its synergism with some antibiotics on *Klebsiella pneumonia* isolated from UTI of pregnant women, *Res. J. Biotech.*, **18(1)**, 29-35 (2023)
7. Barabadi H., Alizadeh Z. and Rahimi M.T., Nanobiotechnology as an emerging approach to combat malaria: a systematic review Nanomedicine, *Nanotechnology, Biology and Medicine*, **18**, 221–233 (2019)
8. Bello O.S. and Ahmad M.A., Coconut (*Cocos nucifera*) shell based activated carbon for the removal of malachite green dye from aqueous solutions, *Sep Sci Technol*, **47**, 903–912 (2012)
9. Bello O.S., Adelaide O.M., Hammed M.A. and Popoola O.A.M., Kinetic and equilibrium studies of methylene blue removal from aqueous solution by adsorption on treated sawdust, *Maced J Chem Chem Eng*, **29**, 77–85 (2010)
10. Chitra M., Kistan A., Kanchana V. and Jayanthi A., Sol-Gel synthesis, characterization and photocatalytic activity of Cobalt doped ZnO nanoparticles, *Res. J. Chem. Environ.*, **28**, 3 (2024)
11. Chieng H.I., Lim L.B.L. and Priyanantha N., Sorption characteristics of peat from Brunei Darussalam for the removal of rhodamine B dye from aqueous solution: adsorption isotherms, thermodynamics, kinetics and regeneration studies, *Desalin Water Treat*, **55**, 664-672 (2015)
12. Ghaedi M., Nasab A.G., Khodadoust S., Rajabi M. and Azizian S., Application of activated carbon as adsorbents for efficient removal of methylene blue: kinetics and equilibrium study, *J. Ind. Eng. Chem*, **20**, 2317-2324 (2014)
13. Gietu Yirga A., Adugna Nigatu A., Adere Tarekegne H. and Desiew Mekuanint G., Adsorptive removal of malachite green dye from aqueous solution onto activated carbon of *Catha edulis* stem as a low cost bio-adsorbent, *Environ Syst Res*, **9**, 29 (2020)
14. Gomathi M., Prakasam A. and Rajkumar P.V., Green Synthesis Characterization and Antibacterial Activity of Silver Nanoparticles Using *Amorphophallus Paeoniifolius* Leaf Extract, *J. Clust. Sci.*, **30**, 995–1001 (2019)
15. Gupta, V.K., Srivastava S.K. and Mohan D., Equilibrium uptake, sorption dynamics, process optimization and column operations for the removal and recovery of malachite green from wastewater using activated carbon and activated slag, *Ind. Eng. Chem. Res*, **36**, 1-10 (2207)
16. Hamelian M., Zangeneh M.M., Amisama A., Varmira K. and Veisi H., Green synthesis of silver nanoparticles using *Thymus kotschyanus* extract and evaluation of their antioxidant, antibacterial and cytotoxic effects, *Appl. Organomet. Chem.*, **32**, e4458 (2018)
17. Islam M.D.J., Khatun M.T., Rahman M.D.R. and Alam M.M., Green synthesis of copper oxide nanoparticles using *Justicia adhatoda* leaf extract and its application in cotton fibers as antibacterial coatings, *AIP Advances*, **11**, 125223 (2021)
18. Jitendra K.S., Shaheer M.A., Ameen S., Pratibha S. and Gurdip S., Green synthesis of CuO nanoparticles with leaf extract of *Calotropis gigantea* and its dye-sensitized solar cells applications, *Journal of Alloys and Compounds*, **632**, 321–325 (2015)
19. Jayalakshmi A.Y., Green synthesis of copper oxide nanoparticles using aqueous extract of flowers of *Cassia alata* and particles characterization, *International Journal of Nanomaterials and Biostructures*, **4**, 66–71 (2014)
20. Kanchana V. and Kistan A., Confiscation of chemical oxygen demand from groundwater samples collected from near tanneries using activated carbon of *Ricinus Communis* blended with coconut shell, *Indian Journal of Environmental Protection*, **40**, 527-532 (2020)
21. Kistan A., Kanchana V., Sakayasheela L. and Sumathi J., Titanium dioxide as a Catalyst for Photo-degradation of Various Concentrations of Methyl Orange and Methyl Red dyes using Hg Vapour Lamp with Constant pH, *Oriental Journal of Chemistry*, **34**, 2 (2018)
22. Kistan A. and Kanchana V., Silver-Alumina Impregnated Maghemite/Magnetite Nanocomposites for Effective Removal of Chromium (VI) from the Tannery Discharge, *Asian Journal of Chemistry*, **35**, 1899-1906 (2023)
23. Kistan A., Kanchan V., Mohan S. and Chitra M., Innovative synthesize of zrO₂ nanomaterial using biodegradable dragon fruit peel extracts and its photocatalytic activity against methyl Orange by UV radiation, *Rasayan Journal of Chemistry*, **17**, 199-206 (2024)
24. Kumar V., Bano D., Mohan S., Singh D.K. and Hassan S.H., Sunlight induced Green synthesis of silver nanoparticles using aqueous leaf extract of *longifolia* and its antioxidant activity, *Mater. Lett*, **181**, 371-377 (2016)

25. Lee S.L., Park J.H., Kim S.H., Kang S.W., Cho J.S., Jeon J.R., Lee Y.B. and Seo D.C., Sorption behavior of malachite green onto pristine lignin to evaluate the possibility as a dye adsorbent by lignin, *Appl Biol Chem*, **62**, 3 (2019)

26. Mohan S., Kistan A., Mahalakshmi S., Jayanthi A., Ramya A. and Karthik Siva P., Sol-Gel technique, characterization and photocatalytic degradation activity of Manganese doped ZnO nanoparticles, *Main group Chemistry*, **24**, 1-14 (2023)

27. Naika H.R., Lingaraju K., Manjunath K., Kumar D., Nagaraju G., Suresh D. and Nagabhushana H., Green synthesis of copper oxide nanoparticles using Gloriosa superba L. extract and their antibacterial activity, *Journal of Taibah University for Science*, **9**, 7-12 (2015)

28. Nisha Mary U., Venkatesh D., Arulmurgan S., Kistan A., Rajeshwaran P. and Siva Karthik P., Assessment of solar light sensitive Chitosan integrated CeO₂-CuO ternary composites for the efficient degradation of Malachite Green, Acid Blue 113 dyes and microbial studies, *Inorganic Chemistry Communications*, **160**, 111942 (2023)

29. Premkumar A., Kistan A. and Kanchana V., A Simple Treatment of Tannery Wastewater using Modified Activated Carbon by Metal Chloride, *Asian Journal of Chemistry*, **34**, 1698-1702 (2022)

30. Rohani M. and Asmadi A., Removal of Malachite Green Dye Using Oil Palm Empty Fruit Bunch as a Low-Cost Adsorbent, *Bio Interface Research in Applied Chemistry*, **11**, 14998-15008 (2021)

31. Sangon S., Hunt A.J., Attard T.M., Mengchang P. and Supanchaiyamat N., Valorisation of waste rice straw for the production of highly effective carbon based on adsorbents for dye removal, *J. Clean. Prod.*, **172**, 1128-1139 (2017)

32. Shah M., Fawcett D., Sharma S., Tripathy S. and Poinern G., Green synthesis of metallic nanoparticles via biological entities, *Materials*, **8**, 7278-7308 (2015)

33. Siddiqui S., Goddard R.H. and Bielmyer-Fraser G.K., Comparative effects of dissolved copper and copper oxide nanoparticle exposure to the sea anemone, *Exaiptasia pallida*, *Aquatic Toxicology*, **160**, 205-213 (2015)

34. Singh A. and Wadhwa N., A Review on Multiple Potential of Aroid: *Amorphophallus Paeoniifolius* Synonyms, *Int. J. Pharm. Sci. Rev.*, **24**, 55-60 (2014)

35. Sivaraj R., Rahman P.K.S.M., Rajiv P., Narendhran S. and Venkatesh R., Biosynthesis and characterization of Acalypha indica mediated copper oxide nanoparticles and evaluation of its antimicrobial and anticancer activity, *Spectrochimica Acta Part A: Molecular and Biomolecular Spectroscopy*, **129**, 255-258 (2014)

36. Vijaya Anandan V.A., Kistan A., Saral A. and Thaminum Ansari A., Retarding of Preliminary Chemical Pollutants from Dye Effluent by Metal Nano Particles Synthesized using Flower Extract of Catharanthus Roseus, *Oriental Journal of Chemistry*, **34**, 81 (2018)

37. Vishveshvar K., Krishnan M.V.A., Haribabu K. and Vishnuprasad S., Green Synthesis of Copper Oxide Nanoparticles Using Ixiro coccinea Plant Leaves and its Characterization, *Bio Nanoscience*, **8**, 554-58 (2018)

38. Wang H., Li Z., Yuan Y., Sun F., Chang H., Deng L., Xie H. and Li, A highly sensitive gas sensor based on CuO nanoparticles synthetized via a sol-gel method, *RSC Adv.*, **6**, 79343-49 (2016)

39. Worku Wubet A., Fedlu Kedir S., Endale Tsegaye M., Hadgu Hailekiros B. and Bedasa Abdisa G., Synthesis of Copper Oxide Nanoparticles Using Plant Leaf Extract of Catha edulis and Its Antibacterial Activity, *Hindawi Journal of Nanotechnology*, **2932434**, 10 (2020)

40. Yallappa S., Manjanna J., Sindhe M.A. and Nagaraja K., Microwave assisted rapid synthesis and biological evaluation of stable copper nanoparticles using T. arjuna bark extract, *Spectrochimica Acta Part A: Molecular and Bio Molecular Spectroscopy*, **110**, 108-115 (2013).

(Received 19th March 2024, accepted 01st June 2024)